A R C H I V E S O F M E T A L L U R G Y A N D M A T E R I A L S
Volume 60 2015 Issue 4
DOI: 10.1515/amm-2015-0460

M. TKADLEČKOVÁ*, K. MICHALEK*, P. MACHOVČÁK**, M. KOVÁČ***, L. SOCHA*

STUDY OF CASTING AND SOLIDIFICATION OF SLAB INGOT FROM TOOL STEEL USING NUMERICAL MODELLING

MODELOWANIE NUMERYCZNE ODLEWANIA I KRZEPNIĘCIA WLEWKÓW STALOWYCH ZE STALI NARZĘDZIOWEJ

The main problem in the production of forgings from tool steels, especially thick plates, blocks, pulleys and rods which are used for special machine components for demanding applications, it is the inhomogeneous structure with segregations, cracks in segregations or complex type of non-metallic inclusions MnS and TiCN. These forgings are actually produced from conventional forging ingots. Due to the size of forgings, it would be interesting the production of these forgings from slab ingots. It is possible that the production of forgings from slab ingots (which are distinguished by a characteristic aspect ratio A/B), it would reduce the occurrence of segregations. The paper presents the verification of the production process of slab steel ingots in particular by means of numerical modelling using finite element method. The paper describes the pre-processing, processing and post-processing phases of numerical modelling. The attention was focused on the prediction of behavior of hot metal during the mold filling, on the verification of the final porosity, of the final segregation and on the prediction of risk of cracks depending on the actual geometry of the mold.

Keywords: steel, slab ingot, macrosegregation, cracks, modelling

Głównym problemem w produkcji odkuwek ze stali narzędziowych, szczególnie grubych płyt, bloków, kół pasowych i prętów, używanych do specjalnych elementów maszyn dla żądanych zastosowań, jest niejednorodna struktura z segregacją, pęknięciami w segregacji lub złożonego typu niemetaliczne wtrącenia MnS i TiCN. Te odkuwki są rzeczywiście produkowane z konwencjonalnych wlewków przeznaczonych do kucia. Ze względu na wielkość odkuwek, można by produkować te odkuwki z wlewków płaskich. Możliwe, że produkcja odkuwki z wlewków płaskich (które wyróżniają się charakterystycznym stosunkiem A/B), pozwoli zmniejszyć występowanie segregacji. W pracy przedstawiono weryfikację procesu produkcji wlewków płaskich za pomocą modelowania numerycznego z wykorzystaniem metody elementów skończonych. Artykuł opisuje fazy modelowania numerycznego: wstępną fazę przetwarzania, obróbkę i przetwarzanie końcowe. Zwrócono uwagę na zachowanie się ciekłego metalu podczas napełniania wlewnic, na weryfikację końcowej porowatości, końcowej segregacji i przewidywania ryzyka pęknięcia w zależności od rzeczywistej geometrii wlewnic.

1. Introduction

Forged thick steel plates, blocks, pulleys and rods are widely used for special machine components for demanding applications. These forgings must have very high qualities free of shrinkage, porosity, segregation, cracks, etc. Actually, these forgings are obviously produced from conventional forging heavy ingots where we can expect a typical non-uniform cast macrostructure of an ingot as well as the macrostructure, which is the result of plastic deformation during the subsequent process of the forming [1-6]. The main precondition of the competitiveness of any steel plant is production of a consistently high quality. For achievement of the high quality of final steel heavy ingots, the electro-slag remelting technology can be used (ESR). ESR ingots have uniform composition and dense structure, but not only the production cycle is long but also energy consumption is high. Such high cost makes ESR not be widely used [7-9].

Therefore, the great effort of steel plants is devoted to development of new non-conventional technologies for manufacturing large ingots, such as for example the intensive water cooling [7], or gradient cooling process (in which the upper part of the ingot is air cooled and the lower part is spray cooled), which can efficiently reduce shrinkage porosity of the ingot by optimizing the solidification sequence, and increase the solidification rate of the ingot [10]. As it is also evidenced by the results of studies performed e.g. by the authors [11-14], the size of the central defect is strongly dependent on the shape of ingot and the hot top.

* VŠB-TECHNICAL UNIVERSITY OF OSTRAVA, FACULTY OF METALLURGY AND MATERIALS ENGINEERING, DEPARTMENT OF METALLURGY AND FOUNDRY, AND REGIONAL MATERIALS SCIENCE AND TECHNOLOGY CENTRE, 17. LISTOPADU 15/2172, OSTRAVA-PORUBA, CZECH REPUBLIC

** VÍTKOVICE HEAVY MACHINERY A.S., OSTRAVA, CZECH REPUBLIC

*** MECAS ESI S.R.O., CZECH REPUBLIC

Corresponding author: marketa.tkadleckova@vsb.cz

Due to the size of forgings (thick steel plates, blocks etc.), it would be interesting the production of these forgings from slab ingots. It is possible that the production of forgings from slab ingots (which are distinguished by a characteristic aspect ratio A / B), it would reduce the occurrence of segregations. One of the ways how to monitor and optimize the production steps from the casting to the forming process is the use of methods of numerical modelling [10-20].

In this study, the casting and solidification of heavy slab ingot weighted 40 t from tool steels have been numerically simulated with a finite element method. The attention of numerical modelling was focused on the prediction of behaviour of hot metal during the mould filling, on the verification of the final porosity, of the final segregation and on the prediction of risk of cracks on the actual geometry of the iron mould. Also, the problems with setting of numerical model and with the determination of the thermodynamic properties of materials are discussed.

2. Definition of numerical model

Generally, the numerical solution of each task is divided into three stages: 1. Pre-processing: includes the geometry modelling and the process of generation of the computational mesh, and definition of calculation. 2. Processing: it involves the computation in the solver. 3. Post-processing: it focuses on evaluation of the results.

2.1. Geometry and computational mesh

The large ingots are specific in terms of simulation. Shapes are usually simple, but one must keep in mind the great size of casting and adapt the quality of mesh and definition of simulation.

The first question is to use or not to use symmetry. The geometry usually allows a user to use one or two symmetry planes. For the simulation of filling it is recommended to use the whole geometry. The one reason is that the inlet of metal must be set up in contact with symmetry plane and symmetry plane slightly influences way of ingot filling. The second reason is that the field of velocity vectors is not complete in horizontal cut. For better observation of the metal's behaviour during the mould filling one should use the whole ingot geometry [21].

Also, when large ingots are modelled, the mesh size becomes very large with respect to the thermal gradients, especially in the early stages of cooling. In order to have appropriate answers (i.e. more accurate temperatures), it is advised to generate a few layers (of a few mm in thickness) inside the ingot, as well as inside the mould [22].

In presented case, only the one type of computational mesh for calculation of filling and solidification was used and we calculated the whole process in one step. The reason of using of one type of computational mesh is the prediction of concentrate changes during the macrosegregation calculation. Indeed, if it is computed the production process of ingot in two steps, the initial conditions in the setting of macrosegregation simulation during solidification would be extracted from the phase of the filling. But during the filling, the thin solid crust on the interface of mould and ingot is obviously created. And in this thin solid crust, the macrosegregation it is not possible to compute. The final surface and volume computational mesh of finite tetra elements used in this study is shown on Fig. 1. The average size of the tetra mesh elements was about 30 mm. The total numbers of tetra elements was 1.620.658.

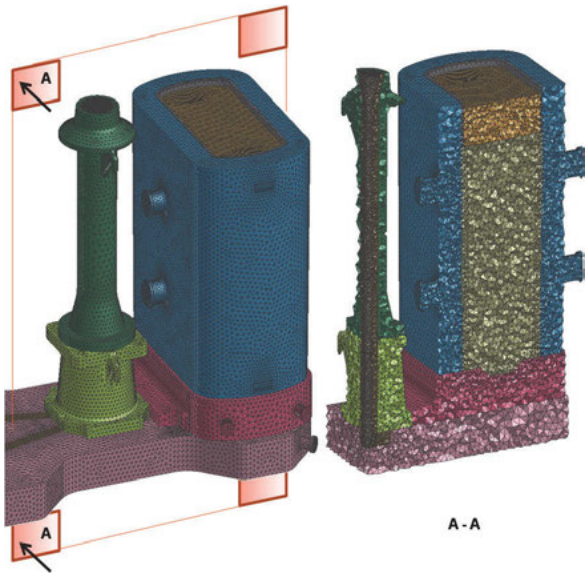

Fig. 1. View on the final geometry and computational surface and volume mesh of the casting system of 40-tons heavy steel slab ingot (The window with symbols „A" introduces the cut plane of view of volume mesh.)

2.2. Material properties

The composition of tested tool steel is given in Tab.1. The mould and the others parts of the casting system was from cast iron. Because the steel and the material of the mould were not included in the basic material database of the simulation programme, the integrated thermodynamic database was used to calculate of thermodynamic properties. The liquidus temperature of the steel was 1,487 ºC, and the solidus temperature was 1,436 ºC. The calculated thermodynamic properties of steel and mould, such as thermal conductivity and enthalpy, are compared in Fig.2.

To achieve relevant numerical results, it is necessary to have correctly defined thermodynamic properties of steel. Therefore, the phase transformation temperatures should be verified using the some different methods. For determination of liquidus and solidus temperature and heat capacity, the thermal analysis can be used [23]. The reason of the verification of the theoretically defined thermodynamic properties is the fact that the thermodynamic database obviously can calculate with the equilibrium state during the determination of phase transformation temperatures. But the steel is a multicomponent heterogeneous material with difficult structure and the metallurgical production process can lead to evolution a many types of non-metallic phases. These non-metallic phases can have different physical properties than the metal matrix which influence the values of phase transformation temperatures and also the character of transformation [23].

2.3. Boundary conditions and interface

The total filling time was 31 minutes. The casting temperature was 1,545 °C. The following equation (1) shows the three possible contributions to the "Heat" boundary condition (all the contributions are added, although they may not be all active in the same time or in the same cases) [22]:

$$Q = Flux + h(T - T_a) + \sigma\varepsilon\left(T^4 - T_a^4\right) \quad (1)$$

where he first term corresponds to a specified flux (***Flux***). It can be used if a given heat flux was measured for instance. The second term corresponds to Convective cooling. This is the most common definition of the cooling of an external face. It is defined by a heat transfer coefficient (***h***) with the ambiance ($\boldsymbol{T_a}$) and by an external temperature (***T***) (of the ambiance). The third term is used at high temperature, when radiation becomes important. In this case, the transfer is proportional to the Stefan-Bolzmann constant ($\boldsymbol{\sigma}$) and the emissivity ($\boldsymbol{\varepsilon}$) and the difference of the fourth power of the temperatures (surface temperature (***T***) and ambiance temperature ($\boldsymbol{T_a}$)). In our case, the heat loss through the surface of the mould was defined as a convective cooling. The ambient temperature was 20 °C, the emissivity was 0.85. On the surface of the steel in a hot top was defined the adiabatic condition. The heat transfer coefficient between mould and ingot was in the range 50 – 1000 $W.m^{-2}K^{-1}$ depending on time (depending on the phase of numerical calculation) [24, 25].

3. Discussion of the achieved results

The results of numerical modelling predicted the character of the steel flow during the filling of the mould, the velocity of the steel flow (which is important for the determination of the cover powder entrainment inside the steel during the casting), the total solidification time, the internal porosity, the macrosegregation of the elements, an in the end the risk of hot tearing and cracks.

3.1. Character of the steel flow

The fluid flow module allows performing mould filling calculation (free surface) as well as fluid flow computation,

TABLE 1

Composition of steel in wt. %

C	Mn	Si	P	S	Cu	Ni	Cr	Mo	Al
0.385	1.45	0.25	0.01	0.005	0.15	1.1	1.975	0.225	0.0125

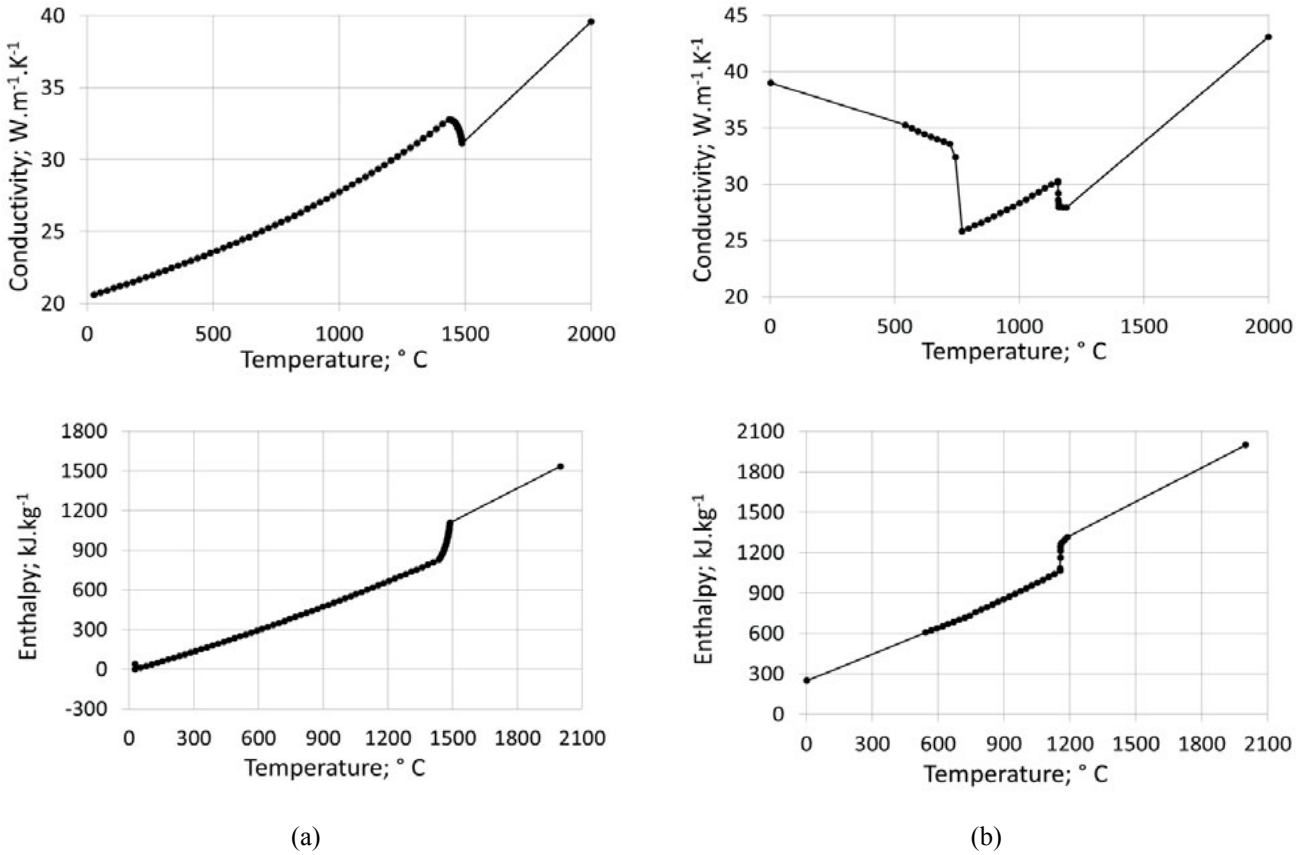

(a) (b)

Fig. 2. Comparison of the calculated thermodynamic properties of steel (column (a)) and mould (column (b))

by the solution of the Navier-Stokes equation. In our case, the bottom filling through two inlets was calculated.

It is evident from Fig.3 (where the character of the steel flow during the filling of the mould is shown using the velocity vectors), that during the casting we can observe the connection of streams. The connection of streams is possible to explain due to a natural convection in this way: near the wall inside of the mould the steel is cooling and because of the higher density, the steel sinks to the bottom of the mould. There the stream of cooler steel is turns to the direction of inlets where the new steel is supplied. The cooler steel is partly mixed with the "new" warmer steel, nevertheless the main streams are due to strong influence of the cooler streams pressed together. In the end, the streams are connected.

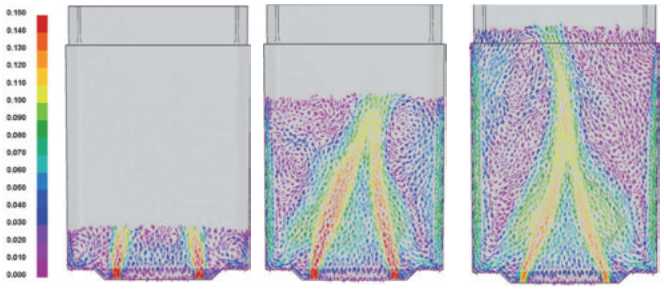

Fig. 3. The character of the steel flow during the bottom filling of the slab mould using velocity vectors in m.s^{-1}

3.2. The velocity of steel flow

The evaluation of the velocity of steel flow during the early stages of the mould filling is very important due to determination of the cover powder entrainment back into the steel melt. The estimated velocity limit was 0.1 m.s^{-1}. The estimated limit introduces the moment when we expect the disconnection of the casting stream from the surface of the casting steel in the mould (and we also expect the reduction of the risk of entrainment of the cover powder back into steel). Based on the established velocity limit, the cut-off function displays a given velocity in specific time which corresponds to some level of the surface of the steel in mould, as it is given on Fig.4. In our case, the distance from the bottom of the mould to the surface level of steel (when we expect the disconnection of the stream) was 1,130 mm. If the hot metal flowing faster than chosen velocity limit in specific time will not reach to the steel surface, we can expect the disconnection of the main stream of the steel and also the lower risk of entrainment of the cover powder. However, the estimation of the velocity limit depends on the practise experience. Therefore, this method of evaluation is appropriate for a comparison of numerical results under various boundary conditions of casting.

Fig. 4. The velocity limit 0.1 m.s^{-1} displays using the cut-off function

3.3. Porosity

The porosity is induced by two mechanisms, solidification shrinkage and gas segregation. The porosity was numerically solved based upon the model developed by Pequet, Gremaud and Rappaz. For further details, please refer to [26, 27].

Fig. 5 shows the final porosity and size of the shrinkage in the hot top. The porosity is shown in numerical results by whole elements (calculation cells) with certain non-filled percent of the metal volume. It means that this not concern the porosity alone. That's why porosity may appear at simulations larger than it will be in reality. In our case, the volume of affected elements of the mesh was 17.544 cm^3. But the volume of microporosity does not exceed the 304 cm^3. Moreover, the microporosity (share of volume of the calculation cell not filled with metal) varied up to do 2 % may be fully eliminated by the following forging.

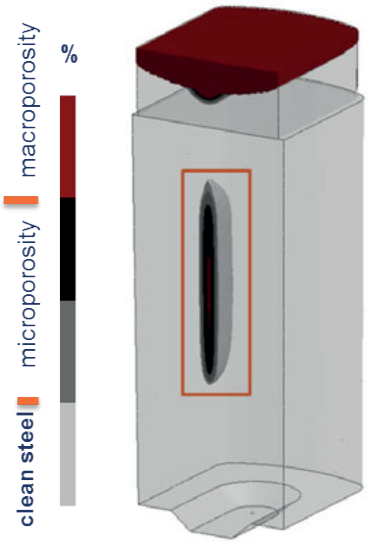

Fig. 5. The character of the predicted microporosity and macroporosity in the steel slab ingot

3.4. Macrosegregation

The computation of macrosegregation was possible due to the MICRO module of the solver. The MICRO module is integrated with thermodynamic parameters of cast materials, such as liquidus temperature and solidus temperature. The liquid species conservation is governed by the equation [20]:

$$f_l \rho_l \frac{\partial c_l^m}{\partial t} + f_l \rho_l \upsilon_l \cdot \nabla c_l^m = \nabla \cdot \left(f_l \rho_l D_l^m \nabla c_l^m \right) + \left(c_l^m - c_{sl}^m \right) \frac{\partial}{\partial t} \left(\rho_s f_s \right) + \frac{S \rho D_s^m}{l} \left(c_s^m - c_{sl}^m \right) \quad (2)$$

The solid species conservation describes the equation (3)

$$f_s \rho_s \frac{\partial c_s^m}{\partial t} = \left(c_{sl}^m - c_s^m \right) \left[\frac{\partial}{\partial t} \left(\rho_s f_s \right) + \frac{S \rho_s D_s^m}{l} \right] \quad (3)$$

where c is concentration, m is species, $l = f_s\ d_2\ /6$ is diffusion length, $S = 2 / d_2$ is interfacial area concentration, d_2 is secondary dendrite arm space, sl is solid and liquid interface and D is diffusivity.

Obviously, the macrosegregation is influenced by the natural convection during solidification – therefore it is recommended to also activate the equations of flow. The temperature dependence of density for liquid metals is linear:

$$\rho^m(T) = \rho_{ref}^m + \left(\frac{\partial \rho}{\partial T} \right)_m \left(T - T_{ref}^m \right) \quad (4)$$

where ρ_{ref}^m is reference density, T_{ref}^m is reference temperature. The liquid density is calculated by equation (5):

$$\rho(T)^{-1} = \sum m \frac{c_l^m}{\rho^m(T)} \quad (5)$$

where c_l^m is liquid concentration. If the macrosegregation is computed, it is necessary to consider these limitations: no solid movement, no grain sedimentation, fully equixed dendrites, no columnar dendrites. The macrosegregation was calculated for carbon, manganese, silicon, phosphorus, cooper, nickel, chromium and molybdenum. Although, the macrosegregation of sulphur was also calculated, the actual macrosegregation model of solver was not able to solve the thousandth content of the sulphur.

The Fig.6 presents a final macrosegregation of phosphorus in the central cross section of the ingot body.

The distribution maps of the others elements were very similar. The distribution maps of macrosegregation of the majority elements increased from the wall of the ingot body to the central axis and from the bottom to the hot top of the ingot. Due to the specific character of the natural convection which was discussed in chapter 3.1 of this paper, the higher content of the elements we can observe in the lower third of the ingot. The highest concentration is cumulated in the hot top of the ingot. On the other hand, the range of macrosegregation is lower than in the case of conventional heavy forging ingots with the same weight and produced from the same steel grade.

3.5. Hot tearing and cracks

The prediction of hot tearing and cracks was calculated by activation of Stress module of the solver. To calculate the stresses which can lead to the hot tearing and cracks, the elasto-plastic parameters of steel has to be also generated during the calculation of thermodynamic properties of the steel. Between these parameters belong the Yield strength, Hardening, Young's Modulus and Thermal Expansion Coefficient. The risk of the hot tearing and cracks was predicted using the Hot Tearing Indicator and Cracks in the postprocessor of the solver. The Hot Tearing Indicator is shown on Fig.7, and the risk of cracks is shown on Fig.8. As it is evident from the Fig.7 and Fig.8, the risk of hot tearing and cracks appears in the corner of the bottom ingot and in the position of transformation of the ingot body to the hot top. The risk of the hot tearing near the bottom of the ingot is caused due to huge thermal gradient in these positions. Also, the places near the central porosity can lead to the hot tearing and cracks because the Elastic Plastic Strain is exhausted.

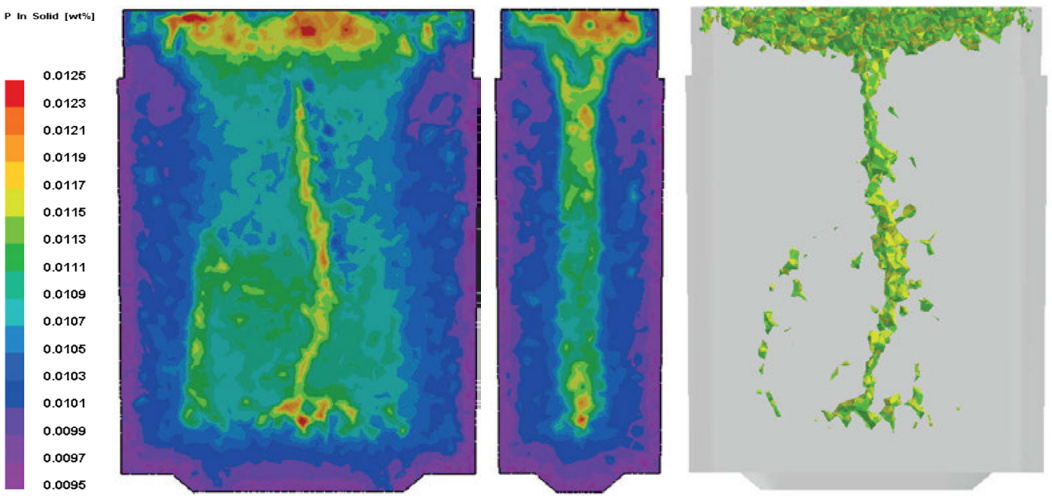

Fig. 6. The distribution map of macrosegregation of phosphorus of 40-tons steel slab ingot (in wt. %). The defined content of phosphorus in the simulation was 0.01 wt. %

Hot Tearing Indicator

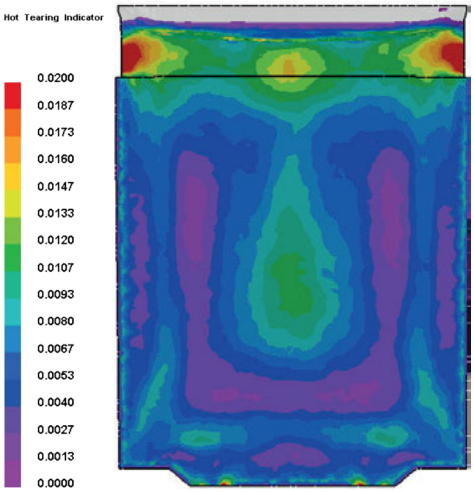

Fig. 7. The prediction of the risk of hot tearing using the Hot Tearing Indicator

Cracking

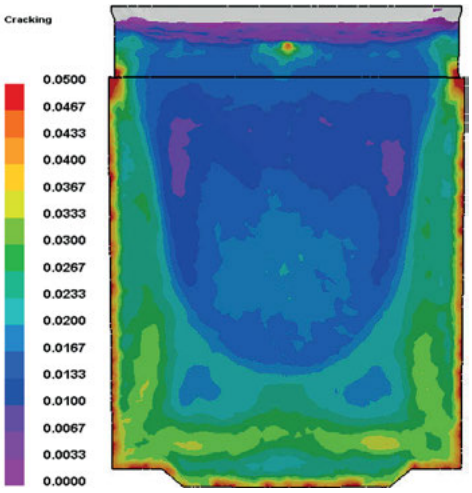

Fig. 8. The prediction of the cracks using the Cracking criterion in postprocessor of the solver

4. Conclusion

The paper was devoted to the verification of the production of the slab ingot from tool steel using the numerical modelling with a finite element method. The main reason of the verification of casting and solidification of the 40-ton steel slab ingot was the possibility of the replacement of the conventional heavy steel ingot actually used for production of the special forgings (such as forged thick steel plates, blocks, pulleys and rods which are widely used for special machine components for demanding applications). In conventional forging heavy ingots, a typical non-uniform cast macrostructure of an ingot we can expect. It is possible that the production of forgings from slab ingots (which are distinguished by a characteristic aspect ratio A / B), it would reduce the occurrence of segregations. Using the numerical modelling, it was found that:

- in slab ingot, we can also expect the typical character of macrostructure with porosity and macrosegregation. But the position of porosity and the size of porosity is more appropriate situated for the forgings such as thick steel plates;
- in the central axis of the ingot body was predicted especially the microporosity, which can be eliminated by the following forging;
- also, the range of macrosegregation is lower than in the case of conventional heavy forging ingots with the same weight and produced from the same steel grade;
- the character of macrosegregation of the majority elements was very similar;
- the prediction of stress properties of the solidified ingot shown that the risk of the hot tearing and cracks is mainly in the bottom corner of the ingot and in the central axis of the ingot near the porosity.

According to these results, the next research will be focused on the verification of the volume defects of this slab ingot under different boundary conditions. Especially, the ratio of A / B, the chamfer and the profile of the mould will be changed.

Acknowledgements

This paper was created with the financial support of TA CR under project No. TA04010035 and in the Project No. LO1203 "Regional Materials Science and Technology Centre - Feasibility Programme" funded by Ministry of Education, Youth and Sports of the Czech Republic.

REFERENCES

[1] M. Kepka, Ovlivňování čistoty oceli, ACADEMIA, Praha, 1986, 156 s. (in Czech)
[2] L. Šmrha, Tuhnutí a krystalizace ocelových ingotů. SNTL, Praha, 1983. ISBN 182664-14825/83 (in Czech)
[3] C. Beckermann, Inter. Mater. Rev. **47**, 243-261 (2002).
[4] J.P. Gu, C. Beckermann, Metall. and Mat. Trans. A **30A**, 1357-1366 (1999).
[5] C. Beckermann, ASM Handbook, Vol. 15, pp 348-352. http://www.engineering.uiowa.edu/~becker/documents.dir/
[6] J. Pieprzyca, T. Merder, M. Warzecha, J. Skorupa, Metalurgija **54**, 127-130 (2015).
[7] Y. Liu, S. Zhou, X. Zhang, M. Geng, Y. Huang In 1st Inter. Conf. on Ingot Casting, Rolling and Forging, Aachen, Germany (2012).
[8] N. Giesselmann, A. Rückert, H. Pfeifer, J. Tewes, J. Klöwer, In 1st Inter. Conf. on Ingot Casting, Rolling and Forging, Aachen, Germany (2012).
[9] YW. Dong., ZH. Jiang, YL. Cao, A. Yu, D. Hou, Metall. and Mater. Trans. B **45**, 1315-1324 (2014).
[10] L. Nan, J. Yonglong, L. Shengli, A. Xingang, Y. Xiaoguang. Research & Development – Chine Foundry 10, 87-91 (2013).
[11] K. Tashiro, S. Watanabe, I. Kitagawa, I. Tamura, ISIJ Int., 312-321 (1983).
[12] A. Kermanpus, M. Eskandari, H. Purmohamad, M.A. Soltani, B. Shateri, Mater. & Design **31**, 1096-1104 (2010).
[13] O. Bogdan, Industrial Soft, Montreal, Canada (2010), http://castingsnet.com/AISI4340-casting-report.pdf
[14] M. Kearney, M. Crabbe, J. Talamantes-Silva, Ironmaking

& Steelmaking, 34, 380-383 (2007).
[15] P. Lan, JQ Zhang, Ironmaking & Steelmaking, **41**, 598-606 (2014).
[16] D. Mazumdar, J.W. Evans, J., W. Modeling of Steelmaking Processes. CRC Press, 1 edition, 2009. ISBN-13: 978-1-4200-6243-4
[17] QY Meng, FM Wang, CR Li, ML Li, J. Zhang, GJ Cui, JOM, 66, 1166-1174 (2014).
[18] WS Li, HF Shen, X. Zhang, BC Liu. Metallur. & Mater. Transac. B **45**, 464-471 (2014).
[19] P. Machovčák, A. Opler, M. Tkadlečková, K. Michalek, K. Gryc, V. K utIs, M. Kováč, In 1st Intern. Confer. on Ingot Casting, Rolling and Forging ICRF, Aachen, Germany (2012).
[20] M. Tkadlečková, P. Machovčák, K. Gryc, K. Michalek, L. Socha, P. Klus, Archiv. of Metall. and Mater. **58**, 171-177 (2013).
[21] Large castings – ingot. Procast 2010. User Guide.
[22] ProCAST 2009, User Guide.
[23] B. Smetana, M. Žaludová, M. Tkadlečková, J. Dobrovská, S. Zlá, K. Gryc, P. Klus, K. Michalek, P. Machovčák, L. Řeháčková, Journal of Therm. Anal. & Calorim. 112, 473-480 (2013).
[24] M. Tkadlečková, K. Gryc, L. Socha, K. Michalek, P. Klus, P. Machovčák, In: 21st Intern. Confer. on Metall. and Mater. METAL 2012, Brno, Czech Republic, EU. 59-65, 2012. ISBN 978-80-87294-31-4.
[25] M. Tkadlečková, K. Gryc, P. Machovčák, P. Klus, K. Michalek, L. Socha, M. Kováč. Mater. in Technol. **46**, 399-402 (2012).
[26] Ch. Pequet, M. Gremaud, M. Rappaz, Met. Mater. Trans. **33A**, 2095-2106 (2002).
[27] G. Couturier, M. Rappaz, Model. and Simul. in Mater. Scien. and Engin. **14**, 253-271 (2006).

Received: 20 October 2014.